Reading the Fold

A Global Newton Series for the Riemann Xi Function

Jeffery Huckstead
Cerebral Graphix — CerebralGraphix.com

Version 1.3 · 20 October 2026 · DOI 10.5281/zenodo.23511096

Abstract

The triangular coordinate $q = s(1-s) = -2T(s-1)$ folds the two arguments s and $1-s$ related by the functional equation of the completed Riemann function ξ into one, so $\xi(s) = X(q)$ for a single entire function X. The critical line becomes the ray $q \geq \frac{1}{4}$, and the real axis beyond $s = 1$ becomes the negative axis. We sample X at $q = -j$ for $j = 0, 1, 2, \ldots$, that is at the real points $s_j = (1 + \sqrt{1+4j})/2$, and take finite differences. Every forward difference η_n is strictly positive, and the Newton series

$$X(q) = \sum_{n \geq 0} (-1)^n \eta_n \, \frac{q(q+1)\cdots(q+n-1)}{n!}$$

converges absolutely and locally uniformly on the whole complex plane. Its basis is the rising-simplex hierarchy $1,\ q,\ T(q),\ \ldots$, so the triangular polynomial appears both as the coordinate and in the basis.

Geometrically, the fold is a parabola. With $J = 2s - 1$, the identity $J^2 = 8T(s-1) + 1$ is the square of side J split into eight triangles around one centre, and $q = (1 - J^2)/4$. Real J carries the samples, imaginary J carries the critical line, and the two branches meet at the vertex $q = \frac{1}{4}$.

The coefficients fall at the sharp rate $n\,\eta_n^{1/n}/(\ln n)^2 \to e/16$, and the next two logarithmic corrections are determined exactly. A contour remainder gives fully rational error bounds for every finite reconstruction. With 101 coefficients, the exact interpolating polynomial is within 10^{-122} of X on the disk $|q| \leq 201$, which contains the first zeta zero. An interval-certified polynomial with exact rational coefficients is within 4.689×10^{-123} on the same disk.

The same averaging rule that produces the basis also proves the positivity. It places the expansion in a family with Taylor's series, Euler–Maclaurin and a triangular Bernoulli family, which Burnol's recent framework makes precise. Coefficient positivity is unconditional. The determinant conditions equivalent to the Riemann hypothesis are not touched, and we state exactly where they sit.

Contents

1. Introduction **2**
1.1 What is read, and from where . . . 2
1.2 The results in brief . . . 3
1.3 How the paper is arranged . . . 4

2. The fold **4**
2.1 The coordinate . . . 4
2.2 The sampling nodes . . . 5
2.3 The fold as a square and a parabola . . . 5

3. The simplex basis and Newton's differences **7**
3.1 The basis . . . 7
3.2 The averaging rule behind the differences . . . 7
3.3 Newton's series as a non-stationary Taylor expansion . . . 8

4. The global Newton theorem **9**
4.1 The positive source . . . 9
4.2 Proof of Theorem A . . . 9

5. How fast the coefficients fall **10**
5.1 Two inequalities . . . 10
5.2 The root scale $e/16$ . . . 11
5.3 The next two corrections . . . 11
5.4 What the scale does not say . . . 12

6. A finite reconstruction with a rational error bound **12**
6.1 The table . . . 12
6.2 From a truncation bound to a certified value . . . 14
6.3 A certified polynomial . . . 14

7. Four averaging rules **15**

8. What the expansion does not decide **18**
8.1 Two coefficient systems . . . 18
8.2 The determinant criterion . . . 18
8.3 The same basis in other hands . . . 19
8.4 A boundary in the literature . . . 20

9. Around the fold **20**
9.1 Burnol's other theorem: digit sums with modes 91, 991, 9991 . . . 20
9.2 The even nodes and the zeta ladder . . . 21

10. Status of the results **22**

Acknowledgments and methods **23**

References **23**

1. Introduction

1.1 What is read, and from where

The completed Riemann function

$$\xi(s) = \tfrac{1}{2}\, s(s-1)\, \pi^{-s/2}\, \Gamma(s/2)\, \zeta(s)$$

is entire and satisfies $\xi(s) = \xi(1-s)$. Its zeros are the nontrivial zeros of ζ. The Riemann hypothesis says they all lie on the critical line $\operatorname{Re} s = \frac{1}{2}$.

The symmetry suggests a coordinate that cannot tell s from $1-s$. The triangular polynomial $T(z) = z(z+1)/2$ supplies one:

$$q = s(1-s) = -2T(s-1) = \frac{1-J^2}{4}, \qquad J = 2s-1.$$

Reflection is $J \mapsto -J$, which leaves q fixed. So ξ descends to an entire function X with $\xi(s) = X(q)$. Two readings of ξ now share one real line (Figure 1):

- **The critical line becomes a ray.** If $s = \frac{1}{2} + it$, then $q = \frac{1}{4} + t^2$. Every zero on the critical line is a real point $q \geq \frac{1}{4}$.
- **The real axis past $s = 1$ becomes the negative axis.** If $s > 1$ is real, then $q < 0$. The value $X(-j)$ at a negative integer is $\xi(s_j)$, where

$$s_j = \frac{1 + \sqrt{1 + 4j}}{2}, \qquad j = 2T(s_j - 1).$$

  These are real points on the sheet $s \geq 1$, where ξ is positive and easy to compute. The integers $s = 2, 3, 4, \ldots$ occur at $j = 2T(s-1) = 2, 6, 12, \ldots$.

This paper reconstructs the whole function X, including its values on the critical-line ray, from the real samples $X(0), X(-1), X(-2), \ldots$. The reconstruction comes with a complete error bound.

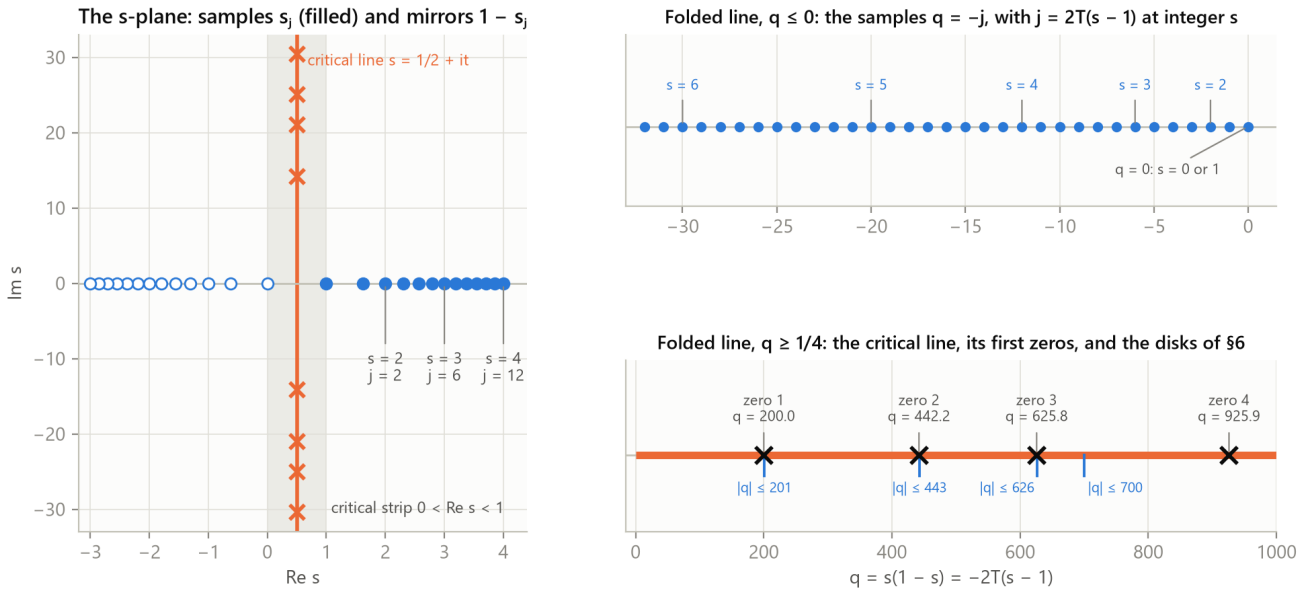

Figure 1: The fold. Left: the s-plane, with the real samples s_j (filled), their mirror images $1 - s_j$ (open) and the first zeros on the critical line. Right: the folded line. The samples fill the negative integers $q = -j$, the critical line becomes the ray $q \geq \frac{1}{4}$, and the zeros sit at $q = \frac{1}{4} + t^2$. The disks $|q| \leq Q$ used in §6 are marked.

1.2 The results in brief

Write $x = -q = s(s-1)$ and $F(x) = X(-x) = \xi\left(\frac{1}{2} + \sqrt{\frac{1}{4} + x}\right)$, so that $F(j) = \xi(s_j)$. Define the forward differences

$$\eta_n = \Delta^n F(0) = \sum_{j=0}^{n} (-1)^{n-j} \binom{n}{j} \xi(s_j).$$

Write $q^{\overline{n}} = q(q+1)\cdots(q+n-1)$, with $q^{\overline{0}} = 1$.

Theorem A (global Newton series). Every η_n is strictly positive, with $\eta_0 = \frac{1}{2}$. The series

$$F(x) = \sum_{n \geq 0} \eta_n \binom{x}{n}, \qquad X(q) = \sum_{n \geq 0} (-1)^n \eta_n \frac{q^{\overline{n}}}{n!}$$

converge absolutely and uniformly on every compact subset of $\mathbb{C}$.

Theorem B (how fast the coefficients fall). With $\ell_1 = \ln n$ and $\ell_2 = \ln\ln n$,

$$\ln \eta_n = -n\ell_1 + 2n\ell_2 + (1 - \ln 16)\, n - \frac{2n\ell_2}{\ell_1} + 2\Big(\ln\frac{2}{\pi} - 1\Big)\frac{n}{\ell_1} + O\Big(\frac{n\ell_2^2}{\ell_1^2}\Big).$$

In particular $n\,\eta_n^{1/n}/(\ln n)^2 \to e/16$.

Theorem C (finite reconstruction with a proved error). Let $P_K(x) = \sum_{n\le K} \eta_n \binom{x}{n}$. Then for $Q > 0$ and $R > \max(K, Q)$,

$$\sup_{|q|\le Q} \big|X(q) - P_K(-q)\big| \le \frac{R}{R-Q}\, F(R)\, \frac{Q(Q+1)\cdots(Q+K)}{(R-K)^{K+1}}.$$

For $K = 100$ this exact-interpolant bound is below 10^{-122} on $|q| \le 201$, a disk containing the first zeta zero. A certified version of P_{100}, with exact rational coefficients, is within 4.689×10^{-123} there (§6).

All three theorems are unconditional; none uses information about where the zeros are. The Riemann hypothesis is equivalent to a family of determinant inequalities for the Taylor coefficients of F, and §8 explains why positivity of single coefficients does not reach it.

1.3 How the paper is arranged

- §2 sets out the fold and its sampling nodes, and reads the fold geometrically as a square and a parabola.
- §3 introduces the rising-simplex basis and the averaging rule that turns it into Newton's series.
- §4 proves Theorem A.
- §5 proves Theorem B.
- §6 derives Theorem C, its numerical table and the certified polynomial.
- §7 places the expansion in a family of four averaging rules: Taylor, Euler–Maclaurin, a triangular rule and Newton. It ends with the entropy of the reciprocal-triangular law and of the fold's two-outcome case.
- §8 states what the expansion does not decide.
- §9 follows the same operator into Burnol's digit-restricted harmonic sums and into the even zeta values at the nodes.
- §10 lists the status of every result.

2. The fold

2.1 The coordinate

The triangular numbers begin with a discrete primitive, $T_n - T_{n-1} = n$, and continue as the polynomial $T(z) = z(z+1)/2$. At $z = s - 1$,

$$T(s-1) = \frac{s(s-1)}{2} = \frac{J^2 - 1}{8}, \qquad q = -2T(s-1) = s(1-s).$$

The map $s \mapsto q$ is two-to-one. It identifies s with $1 - s$, and its only critical point is the centre $s = \frac{1}{2}$, where $q = \frac{1}{4}$. The inverse branch used throughout is

$$s = \tfrac{1}{2} + \sqrt{\tfrac{1}{4} - q}.$$

Because $\xi(s) = \xi(1-s)$, the choice of square-root branch does not matter, and $X(q) = \xi(s)$ is entire in q.

region in s	image in q
critical line $s = \frac{1}{2} + it$	ray $q = \frac{1}{4} + t^2 \geq \frac{1}{4}$
real segment $0 \leq s \leq 1$	segment $0 \leq q \leq \frac{1}{4}$
real $s > 1$ (and its mirror $s < 0$)	negative axis $q < 0$
zero $\rho = \frac{1}{2} + i\gamma$	real point $q_\rho = \frac{1}{4} + \gamma^2$

The first four zeros fold to $q = 200.04$, 442.18, 625.79 and 925.92.

2.2 The sampling nodes

The samples are taken at $q = -j$ for $j = 0, 1, 2, \ldots$, that is at $s_j = \frac{1}{2} + \sqrt{\frac{1}{4} + j}$. The first is $s_0 = 1$, where $\xi(1) = \frac{1}{2}$. Every later node lies on the real sheet $s > 1$. The node j is an integer s exactly when $j = s(s-1) = 2T(s-1)$, so the integers $s = 2, 3, 4, 5, 6$ sit at $j = 2, 6, 12, 20, 30$.

At the even integers the samples are Euler's values, since $\zeta(2k)$ is a rational multiple of π^{2k}:

node $j = 2T_{2k-1}$	$s = 2k$	$F(j) = \xi(2k)$
2	2	$\pi/6$
12	4	$\pi^2/15$
30	6	$2\pi^3/63$
56	8	$4\pi^4/225$
90	10	$8\pi^5/693$

The remaining samples are evaluated numerically from the definition of ξ. Every sample is positive and can be enclosed to any prescribed accuracy; §6.3 encloses the first 101.

2.3 The fold as a square and a parabola

The fold has a direct picture (Figure 2). Ring by ring, a square of side $2n + 1$ splits into eight triangular blocks of T_n sites around one centre site:

$$(2n + 1)^2 = 8T_n + 1.$$

Each ring $k = 1, \ldots, n$ gives k sites to every block. With n replaced by $z = s - 1$, the side $2z + 1$ becomes $J = 2s - 1$, so

$$J^2 = 8T(s-1) + 1, \qquad q = -2T(s-1) = \frac{1 - J^2}{4}.$$

The fold is this square's area read as a parabola in J. The reflection $s \mapsto 1 - s$ is $J \mapsto -J$, the half-turn of the square about its centre, and it leaves every block, and so q, unchanged.

The parabola has two branches, one over real J and one over imaginary J, and they carry the two readings of §1:

- **Real J.**
  - $|J| \geq 1$ gives $q \leq 0$. The samples sit at $J = \pm\sqrt{1 + 4j}$, where $q = -j$.
  - $|J| < 1$ gives $0 < q \leq \frac{1}{4}$. Splitting a square into two staircases, $n^2 = T_n + T_{n-1}$, and putting $s = T_n/n^2$ gives $J = 1/n$ and $q = \frac{1}{4} - 1/(4n^2)$. These points climb to the vertex.
- **Imaginary $J = 2it$.** This gives $q = \frac{1}{4} + t^2$, the critical line. Its zeros sit at $q_\rho = \frac{1}{4} + \gamma^2$.

The two branches meet only at the vertex $q = \frac{1}{4}$, the image of $s = \frac{1}{2}$. Theorem A reconstructs X on the whole q-plane from the values on the first branch.

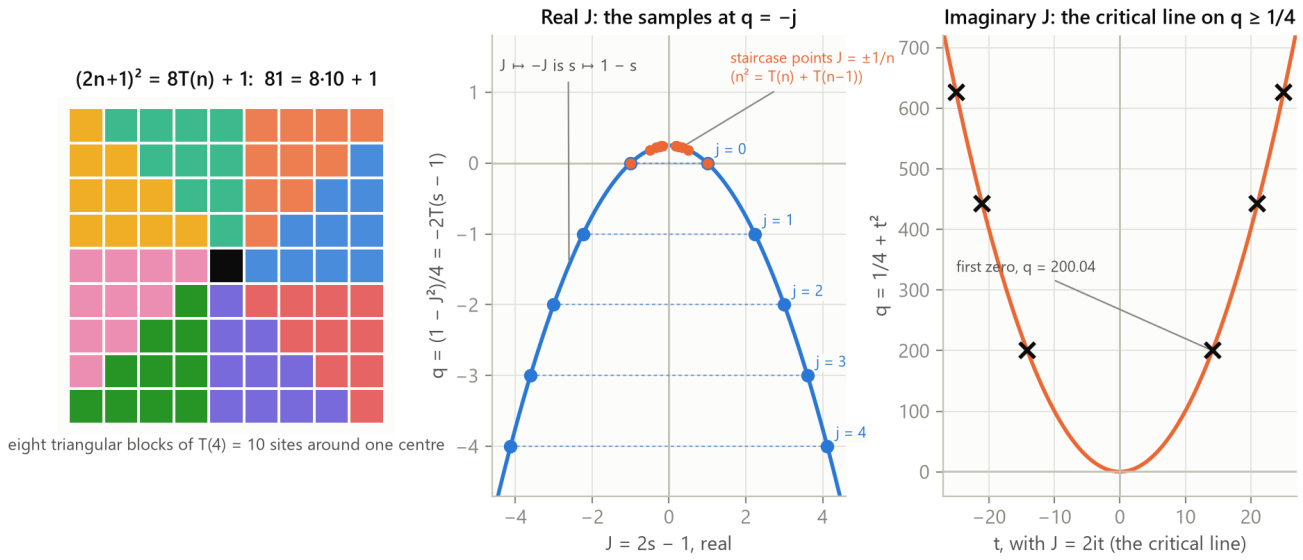

Figure 2: The fold as a square and a parabola. Left: the square of side $2n + 1 = 9$ as eight triangular blocks of $T_4 = 10$ sites around one centre, $81 = 8 \cdot 10 + 1$. Middle: $q = (1 - J^2)/4$ on real $J = 2s - 1$. The samples $q = -j$ sit at $J = \pm\sqrt{1 + 4j}$; the staircase points $J = \pm 1/n$ (orange) climb to the vertex $q = \frac{1}{4}$; $J \mapsto -J$ is the reflection $s \mapsto 1 - s$. Right: the same parabola on imaginary $J = 2it$, which is the critical line $q = \frac{1}{4} + t^2$, with its first zeros.

The half index. At the vertex the side of the square is $J = 0$: the half index $s - 1 = -\frac{1}{2}$, where $T(-\frac{1}{2}) = -\frac{1}{8}$ and $8T(-\frac{1}{2}) + 1 = 0$. Centred there, $T(z) = u^2/2 - \frac{1}{8}$ with $u = z + \frac{1}{2}$. At $z = s - 1$ this is $u = s - \frac{1}{2}$, so that $J = 2u$ and $q = \frac{1}{4} - u^2$. The same point organizes the triangular product

$$\Pi_n(y) = \prod_{j=1}^{n} (1 + jy).$$

The coefficient of y^k in $\Pi_n(y)$ is a polynomial $e_k(n)$ of degree $2k$ in n, with $e_1(n) = T_n$. Evaluated at $-\frac{1}{2}$, these polynomials take the values

$$1,\ -\frac{1}{8},\ \frac{1}{128},\ \frac{5}{1024},\ -\frac{21}{32768},\ -\frac{399}{262144},\ \dots,$$

the coefficients of the classical expansion

$$y^{-1/2}\,\frac{\Gamma(1/y + \frac{1}{2})}{\Gamma(1/y + 1)} \sim \sum_{k \geq 0} e_k\big(-\tfrac{1}{2}\big)\, y^k, \qquad y \to 0^+,$$

which governs the central binomial coefficients [13, §5.11]. Indeed $\Pi_n(y) = y^n\,\Gamma(n+1+1/y)/\Gamma(1+1/y)$ for every integer $n \geq 0$. As $y \to 0^+$ the right side has an asymptotic expansion in powers of y whose coefficients are polynomials in n. They agree with $e_k(n)$ at every integer $n \geq 0$, so they agree at $-\frac{1}{2}$ as well, where the right side is the function above. Apart from the displacement u, which returns in §4.1, none of this is used elsewhere in the paper.

3. The simplex basis and Newton's differences

3.1 The basis

The rising-simplex polynomials are

$$p_n(z) = \frac{z^{\overline{n}}}{n!} = \binom{z+n-1}{n}, \qquad p_0 = 1.$$

Their first members are

$$1, \qquad z, \qquad T(z) = \frac{z(z+1)}{2}, \qquad \frac{z(z+1)(z+2)}{6}, \qquad \dots,$$

the simplex numbers of every dimension, read as polynomials (Figure 3). With the backward difference $\nabla f(z) = f(z) - f(z-1)$ they satisfy $\nabla p_n = p_{n-1}$. They vanish at $0, -1, \dots, -(n-1)$, which are exactly the sampling nodes. Every polynomial f of degree at most K therefore has the exact expansion

$$f(z) = \sum_{n=0}^{K} \nabla^n f(0)\, p_n(z).$$

The whole hierarchy is needed. Fixing the quadratic member $T(z)$ alone leaves the higher members free.

3.2 The averaging rule behind the differences

Let M_n be the distribution of $-(U_1 + \cdots + U_n)$ for independent uniform variables on $[0, 1]$, with $M_0 = \delta_0$. Integrating the fundamental theorem of calculus n times gives

$$\nabla^n f(0) = \mathbb{E}\, f^{(n)}(-U_1 - \cdots - U_n) = \int_{-n}^{0} f^{(n)}(z)\, dM_n(z).$$

The measures M_n are the normalized uniform B-splines on $[-n, 0]$: a box, a triangle, and then piecewise polynomials of degree $n-1$. The n-th difference is the average of the n-th derivative under the n-th spline.

The simplex shadow. Geometrically, M_n is the projection of the uniform measure on an n-simplex whose vertices project to $0, -1, \dots, -n$ (Figure 4). This holds for any such simplex: its shadow is the B-spline with knots at the projected vertices (Curry and Schoenberg [16]). For $n = 2$ the shadow of every such triangle, however lopsided, is the same isosceles triangle on $[-2, 0]$, with apex 1 at -1. The square shows the same profile in whole numbers. Reading an $n \times n$ array along its antidiagonals gives the counts $1, 2, \dots, n, \dots, 2, 1$, an isosceles triangle, and its two halves are the staircases $n^2 = T_n + T_{n-1}$ of §2.3.

The cube and the simplex give the same law. Sort the n uniforms as $U_{(1)} < \cdots < U_{(n)}$. Their spacings, together with $U_{(1)}$ and $1 - U_{(n)}$, are uniform on the standard n-simplex. The weighted sum of the spacings that recovers $-\sum_k U_{(k)} = -\sum_k U_k$ sends the vertices to $0, -1, \dots, -n$.

So the coefficient of the n-th simplex polynomial is the average of $f^{(n)}$ over the shadow of an n-simplex. Positivity is visible in the picture: a positive function averaged over a shadow stays positive.

The same identity, read forwards, is the key to positivity in §4:

$$\Delta^n F(0) = \mathbb{E}\, F^{(n)}(U_1 + \cdots + U_n).$$

A difference is an average of a derivative. If every derivative is positive, every difference is positive.

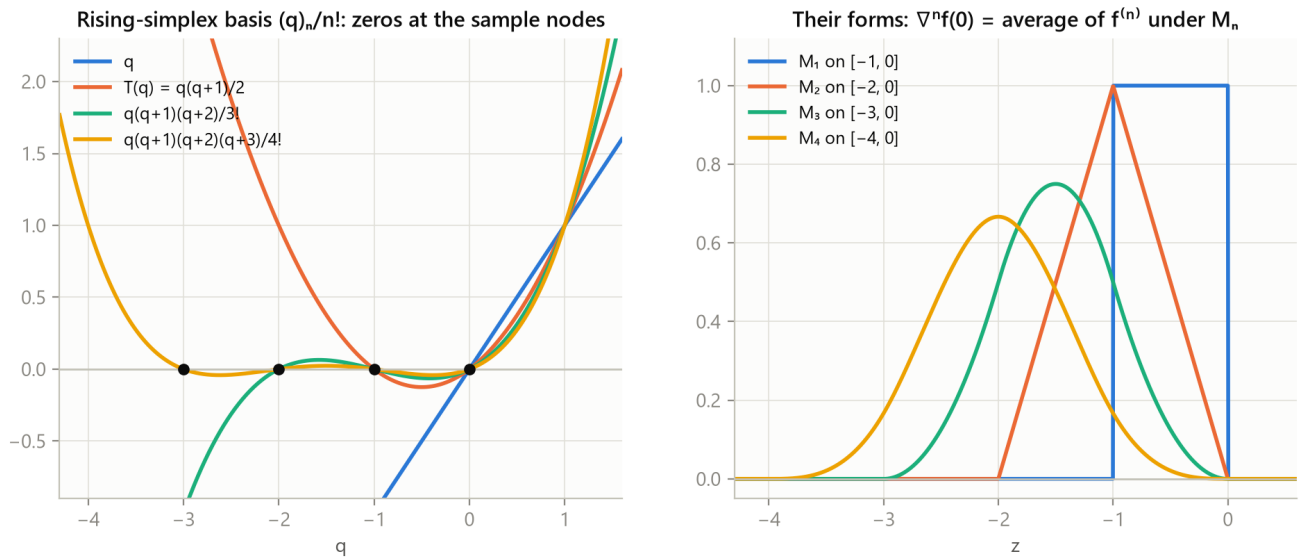

Figure 3: Left: the rising-simplex basis $(q)_n/n!$ for $n = 1, \dots, 4$, whose zeros are the sampling nodes $0, -1, -2, \dots$. All members pass through $(1, 1)$. Right: the forms that produce the coefficients, namely the B-spline shadows M_n of the uniform simplex on $[-n, 0]$. The coefficient of p_n is the average of $f^{(n)}$ under M_n.

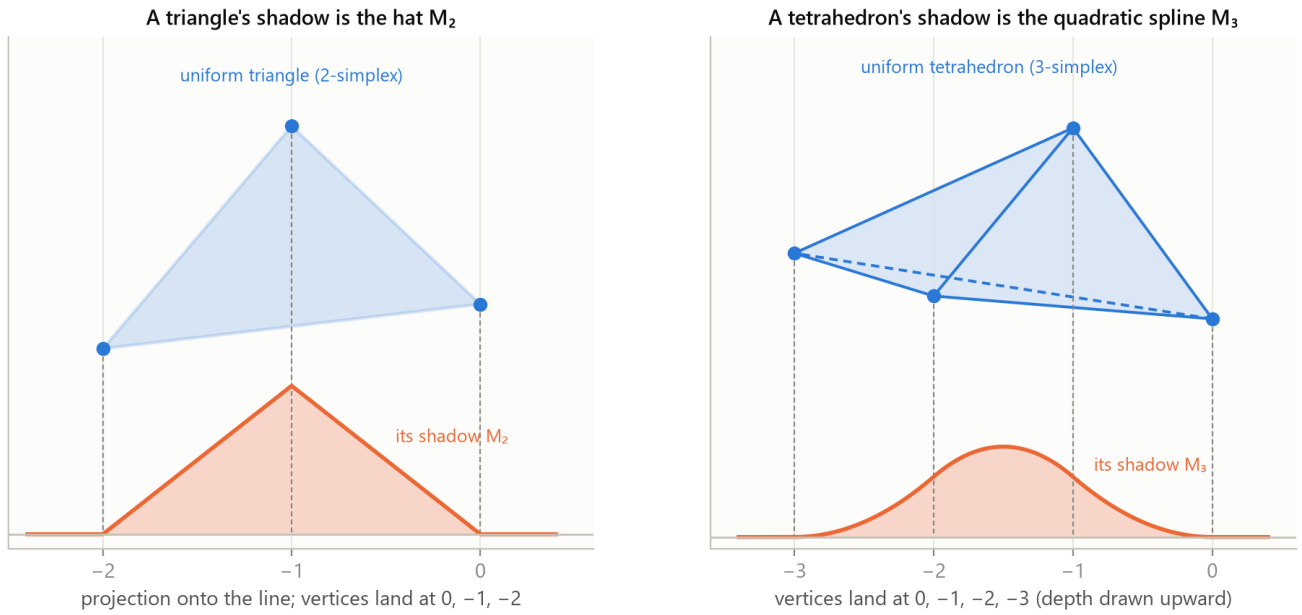

Figure 4: The simplex shadow. Left: a uniform triangle whose vertices project to $0, -1, -2$ casts the hat M_2, an isosceles triangle of base 2, height 1 and area 1, whatever the shape of the triangle above it. Right: a uniform tetrahedron with vertices over $0, -1, -2, -3$ casts the quadratic spline M_3. The projection is along the vertical; depth is drawn upward. The same shadows arise as the laws of $-(U_1 + U_2)$ and $-(U_1 + U_2 + U_3)$.

3.3 Newton's series as a non-stationary Taylor expansion

Burnol has recently set Taylor's formula and the Euler–Maclaurin formula under one roof [3, §§33–35]. Take linear forms $L_1, L_2, \dots$ with $L_j(1) = 1$, and let $I_j\psi = \Psi - L_j(\Psi)$, where Ψ is any antiderivative of ψ. Define

$B_n = n!\, I_1 I_2 \cdots I_n(1)$. Then

$$f(z) = \sum_{j=0}^{n} L_{j+1}\big(f^{(j)}\big)\frac{B_j(z)}{j!} + E_{n+1}(f)(z),$$

with an explicit remainder. When all L_j equal the point mass at a, this is Taylor's formula. When all L_j equal Lebesgue measure on $[0, 1]$, it is the Euler–Maclaurin expansion in Bernoulli polynomials. When the L_j are point masses at varying points, the B_n are Goncharov's polynomials.

The simplex basis is the case

$$L_1 = \delta_0, \qquad L_{n+1} = M_n,$$

in which $B_n/n! = p_n$ and the coefficients become $L_{n+1}(f^{(n)}) = \nabla^n f(0)$. The basis determines these forms on polynomials, so the spline measures are forced by their polynomial moments. Among finite measures on a fixed compact interval they are determined uniquely. Arbitrary unbounded extensions to all continuous functions, which Burnol's first proposition allows, are not determined by the basis.

Newton's backward-difference series is therefore Burnol's non-stationary Taylor–Euler–Maclaurin expansion, driven by the simplex shadows. To apply his finite formula, replace his interval $[0, 1]$ with one that contains the knots $-n, \dots, 0$ and the evaluation point.

An infinite Newton expansion needs more than the identity for polynomials. The function $\sin \pi z$ vanishes at every node without vanishing identically, so its Newton series is zero. When the series does converge to its function, as for

$$e^z = \sum_{n\geq 0} (1 - e^{-1})^n\, p_n(z)$$

(the binomial series), a separate argument is needed. For the folded ξ that argument is Theorem A.

4. The global Newton theorem

4.1 The positive source

The completed function has a classical representation with a positive kernel. In Romik's normalization [1, (1.8), (1.11)],

$$\Phi(v) = 2\sum_{j\geq 1}\big(2\pi^2 j^4 e^{9v/2} - 3\pi j^2 e^{5v/2}\big)e^{-\pi j^2 e^{2v}},$$

and, with $u = s - \frac{1}{2}$ as in §2.3,

$$\xi\big(\tfrac{1}{2} + u\big) = 2\int_0^\infty \Phi(v)\cosh(uv)\, dv = \sum_{k\geq 0} b_k u^{2k}, \qquad b_k = \frac{2}{(2k)!}\int_0^\infty \Phi(v)\, v^{2k}\, dv.$$

For $v \geq 0$ every summand of Φ is positive, because $2\pi j^2 e^{2v} \geq 2\pi > 3$. The kernel decays faster than any exponential as $v \to \infty$. Hence every b_k is positive; see also O'Sullivan [2, (7.1)].

4.2 Proof of Theorem A

Positivity. Since $u^2 = (s - \frac{1}{2})^2 = x + \frac{1}{4}$, the expansion of §4.1 gives

$$F(x) = \sum_{k\geq 0} b_k\big(x + \tfrac{1}{4}\big)^k.$$

So F is entire, and it has positive Taylor coefficients about every real point $x \geq -\frac{1}{4}$. In particular every derivative $F^{(n)}$ is positive on $[-\frac{1}{4}, \infty)$, and by §3.2

$$\eta_n = \Delta^n F(0) = \mathbb{E}\, F^{(n)}(U_1 + \cdots + U_n) > 0.$$

Positivity therefore holds at every order. A finite sign check adds nothing to it.

The remainder. Let $\omega(x) = x(x-1)\cdots(x-K)$. The interpolation polynomial P_K at the nodes $0, \ldots, K$ satisfies the contour formula

$$F(x) - P_K(x) = \frac{1}{2\pi i} \oint_{|w|=R} \frac{F(w)\,\omega(x)}{\omega(w)\,(w-x)}\, dw, \qquad |x| < R,\ R > K.$$

On $|w| = R$ the following bounds hold:

- $|F(w)| \leq F(R)$, because the Taylor coefficients at 0 are positive;
- $|\omega(w)| \geq (R-K)^{K+1}$;
- $|w - x| \geq R - Q$.

For $|x| \leq Q$, $|\omega(x)| \leq Q(Q+1)\cdots(Q+K)$. This gives Theorem C:

$$\sup_{|x|\leq Q} |F(x) - P_K(x)| \leq \frac{R}{R-Q}\, F(R)\, \frac{(Q)_{K+1}}{(R-K)^{K+1}}, \qquad (Q)_{K+1} = Q(Q+1)\cdots(Q+K). \tag{4.1}$$

An explicit value of $F(R)$. At $R = 2a(2a-1)$, for an integer $a \geq 1$, the folded argument is $s = 2a$, so $F(R) = \xi(2a)$. Then $\pi > 3$ and $\zeta(2a) \leq 2a/(2a-1)$ give

$$F\big(2a(2a-1)\big) = \xi(2a) < \frac{2a^2(a-1)!}{3^a}. \tag{4.2}$$

With (4.1), every bound is a rational number whenever Q is rational.

Convergence everywhere. Fix $1 < \alpha < 2$ and take integers $a_K \sim \frac{1}{2}K^{\alpha/2}$, so $R_K = 2a_K(2a_K - 1) \sim K^{\alpha}$. Then (4.2) gives $\ln F(R_K) = o(K \ln K)$. Meanwhile the quotient of products in (4.1) has logarithm $-(\alpha - 1 + o(1))K \ln K$. The remainder therefore tends to zero uniformly on every fixed disk, which proves the expansion of F. Since $X(q) = F(-q)$ and $\binom{-q}{n} = (-1)^n q^{\overline{n}}/n!$, the expansion of X follows. Absolute convergence follows from the coefficient bounds in §5. □

The growth that makes this work is modest: $\ln F(R) = \frac{1}{4}\sqrt{R}\ln R + O(\sqrt{R})$. So F has order $\frac{1}{2}$, with infinite type at that order since $\ln F(R)/\sqrt{R} \to \infty$. It also grows more slowly than any exponential, since $\ln F(R)/R \to 0$.

5. How fast the coefficients fall

5.1 Two inequalities

Positivity and the derivative average give, for every $R > n$,

$$n!\, b_n = \frac{2\,n!}{(2n)!}\, I_n \;\leq\; \eta_n \;\leq\; \frac{n!\, F(R)}{(R-n)^n}, \qquad I_n = \int_0^{\infty} \Phi(v)\, v^{2n}\, dv. \tag{5.1}$$

The left side comes from the single term $k = n$ of the positive expansion. The right side is Cauchy's estimate on circles centred in $[0, n]$.

5.2 The root scale $e/16$

Upper bound. Stirling's formula gives $\ln \xi(s) = \frac{s}{2}\ln s - \frac{s}{2}(1+\ln 2\pi) + O(\ln s)$ as $s \to \infty$, so $\ln F(R) = \frac{1}{4}\sqrt{R}\ln R + O(\sqrt{R})$. Take $R_n = (4n/\ln n)^2$. Then $\ln F(R_n) = 2n + o(n)$ and $\ln(R_n - n) = 2\ln n - 2\ln\ln n + \ln 16 + o(1)$. With $\ln n! = n\ln n - n + o(n)$, the right side of (5.1) gives

$$\ln \eta_n \le -n\ln n + 2n\ln\ln n + (1-\ln 16)\,n + o(n).$$

Lower bound. Keep only the $j = 1$ term of Φ, which gives $\Phi(v) \ge 2\pi(2\pi-3)\,e^{9v/2}e^{-\pi e^{2v}}$ for $v \ge 0$. Restrict the moment integral to an interval starting at $v_n = \frac{1}{2}\ln n - \ln\ln n$, where $e^{2v_n} = n/(\ln n)^2$. This gives $\ln I_n \ge 2n\ln\ln n - 2n\ln 2 + o(n)$. With $\ln\big(n!/(2n)!\big) = -n\ln n + (1-2\ln 2)n + o(n)$, the left side of (5.1) matches the upper bound. Hence

$$\ln \eta_n = -n\ln n + 2n\ln\ln n + (1-\ln 16)\,n + o(n), \qquad \frac{n\,\eta_n^{1/n}}{(\ln n)^2} \to \frac{e}{16}.$$

The two factors of 4 in the 16 have separate sources:

- **From the factorials:** $\big(n!/(2n)!\big)^{1/n} \sim e/(4n)$.
- **From the theta moment:** $I_n^{1/n} \sim (\ln n)^2/4$, because the moment is concentrated near $v \approx \frac{1}{2}\ln n$.

Their product is $e(\ln n)^2/(16n)$.

The constant also depends on the unit sampling step. Fix any $\lambda > 0$ and use unscaled differences, $\eta_n(\lambda) = \Delta_\lambda^n F(0)$ with $\Delta_\lambda F(x) = F(x+\lambda) - F(x)$. Then $\lambda^n n!\, b_n \le \eta_n(\lambda) \le \lambda^n n!\, F(R)/(R-n\lambda)^n$ for $R > n\lambda$, and the same proof gives $n\,\eta_n(\lambda)^{1/n}/(\ln n)^2 \to \lambda e/16$. No uniformity in λ is claimed.

5.3 The next two corrections

Sharpening both bounds determines the next two terms. On the upper side, keep the same radius and retain the n/ℓ_1 terms of the Gamma growth. On the lower side, centre a short interval of length $1/\ell_1$ at

$$v_n = \tfrac{1}{2}\big(\ell_1 - \ell_2 + \ln\tfrac{2}{\pi}\big), \qquad \text{chosen so that } \pi e^{2v_n} = \frac{2n}{\ell_1}.$$

Both sides then agree, for each fixed $\lambda > 0$:

$$\ln \eta_n(\lambda) = n\ln\lambda - n\ell_1 + 2n\ell_2 + (1-\ln 16)n - \frac{2n\ell_2}{\ell_1} + 2\Big(\ln\frac{2}{\pi} - 1\Big)\frac{n}{\ell_1} + O_\lambda\Big(\frac{n\ell_2^2}{\ell_1^2}\Big). \tag{5.2}$$

The coefficient of the first correction is -2, and the next constant is $2(\ln\frac{2}{\pi} - 1) = -2.9031654\ldots$. These are limits of logarithmic corrections; the leading root constant does not change.

This centre approximates the saddle point of the leading exponent. Maximizing $2n\ln v - \pi e^{2v}$ gives $\pi e^{2v} = n/v$, that is $2v\,e^{2v} = 2n/\pi$. So the exact saddle of that exponent is $v_0 = \frac{1}{2}W(2n/\pi)$, where W is the Lambert function, and expanding,

$$v_0 = \tfrac{1}{2}\big(\ell_1 - \ell_2 + \ln\tfrac{2}{\pi}\big) + O(\ell_2/\ell_1).$$

The full integrand also carries the prefactor $e^{9v/2}$ and the higher terms of Φ, which move the true maximum slightly but do not change the error order in (5.2). The 2 in $\ln\frac{2}{\pi}$ comes from the e^{2v} of the theta variable, and the π from the Gaussian exponent $\pi j^2 e^{2v}$. The proof of (5.2) does not need the saddle; it only explains why that centre works.

5.4 What the scale does not say

Define the residual

$$G_n = \frac{n!\,\eta_n}{\left((\ln n)^2/16\right)^n}.$$

By (5.2), $\ln G_n = -2n\ell_2/\ell_1 + O(n/\ell_1) \to -\infty$. So $G_n \to 0$ while $G_n^{1/n} \to 1$. The factorial form

$$\eta_n = \frac{1}{n!}\left(\frac{(\ln n)^2}{16}\right)^n e^{o(n)}$$

is correct, but $e^{o(n)}$ cannot be replaced by $1 + o(1)$, because here it tends to zero. Neither monotonicity nor an onset index is claimed.

The approach to $e/16$ is very slow (Figure 5). The computed coefficients, all positive, are consistent with the formula through $n = 128$, where the scaled root is 0.04361. Evaluating the two-correction formula, without its remainder, gives 0.0466 at $n = 10^2$, 0.1453 at $n = 10^{32}$ and 0.1642 at $n = 10^{192}$. At large n these are values of the asymptotic formula, not of coefficients. The constant was found by analysis; no fit of the finite table would reveal it.

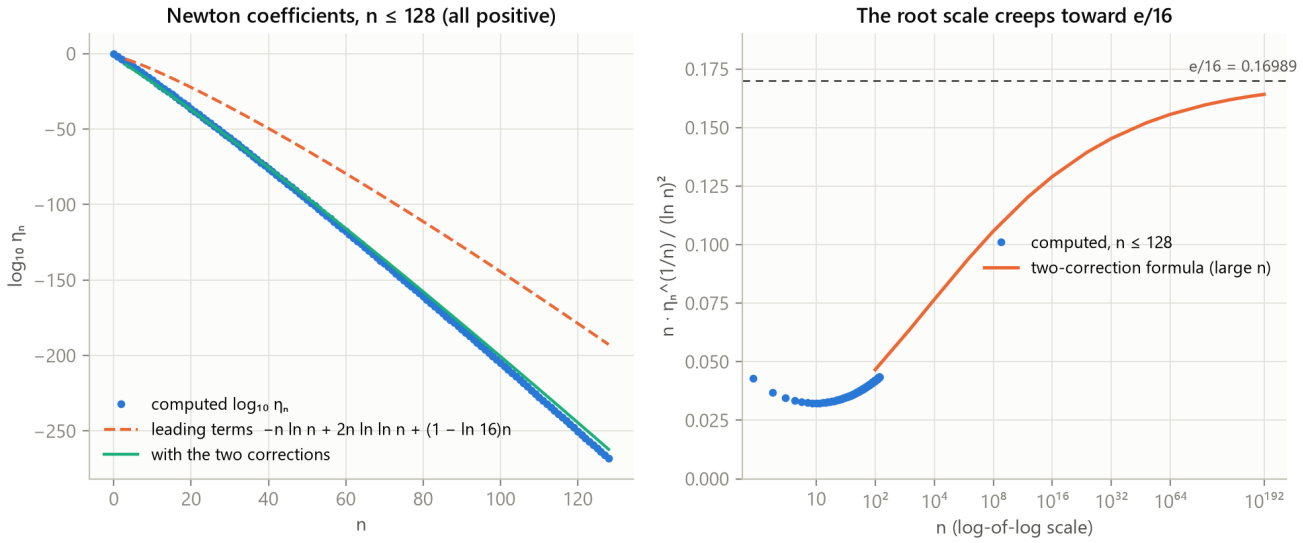

Figure 5: Left: the computed $\log_{10}\eta_n$ for $n \le 128$ (360-digit arithmetic), with the leading terms of (5.2) and with both corrections. Right: the root scale $n\,\eta_n^{1/n}/(\ln n)^2$. The computed values reach 0.0436 at $n = 128$; beyond that the curve is the two-correction formula, evaluated without its remainder, which reaches 0.164 at $n = 10^{192}$ against the limit $e/16 = 0.16989$.

6. A finite reconstruction with a rational error bound

6.1 The table

Take $K = 100$ (101 coefficients, indexed 0 to 100), $a = 66$ and $R = 2a(2a-1) = 17292$ in (4.1) and (4.2). Every quantity is then an integer or a rational number, and exact comparison gives:

disk	largest t on the critical line	covers	proved bound on $\lvert X(q) - P_{100}(-q)\rvert$
$\lvert q\rvert \le \frac{1}{4}$	$t = 0$	centre $s = \frac{1}{2}$ and the segment $0 \le s \le 1$	$< 10^{-206}$
$\lvert q\rvert \le 201$	14.169	first zero ($q = 200.04$)	$< 10^{-122}$
$\lvert q\rvert \le 443$	21.042	second zero ($q = 442.18$)	$< 10^{-92}$
$\lvert q\rvert \le 626$	25.015	third zero ($q = 625.79$)	$< 10^{-78}$
$\lvert q\rvert \le 700$	26.453	the line up to $t = 26.45$	$< 10^{-74}$

The base-10 logarithms of the exact bounds are approximately -206.49, -122.33, -92.49, -78.60 and -74.04.

Figure 6 compares the bounds with the computed reconstruction error at sampled points of the critical line ($t = 0, 0.1, \ldots, 32$). At the last sampled point inside each disk, the computed error is about three orders of magnitude below that disk's proved truncation bound: 2.8, 3.1, 2.9, 2.8 and 3.0 orders. These are samples on one line, not a measured maximum over a complex disk. Larger K extends the reach: the same construction with more coefficients covers more zeros.

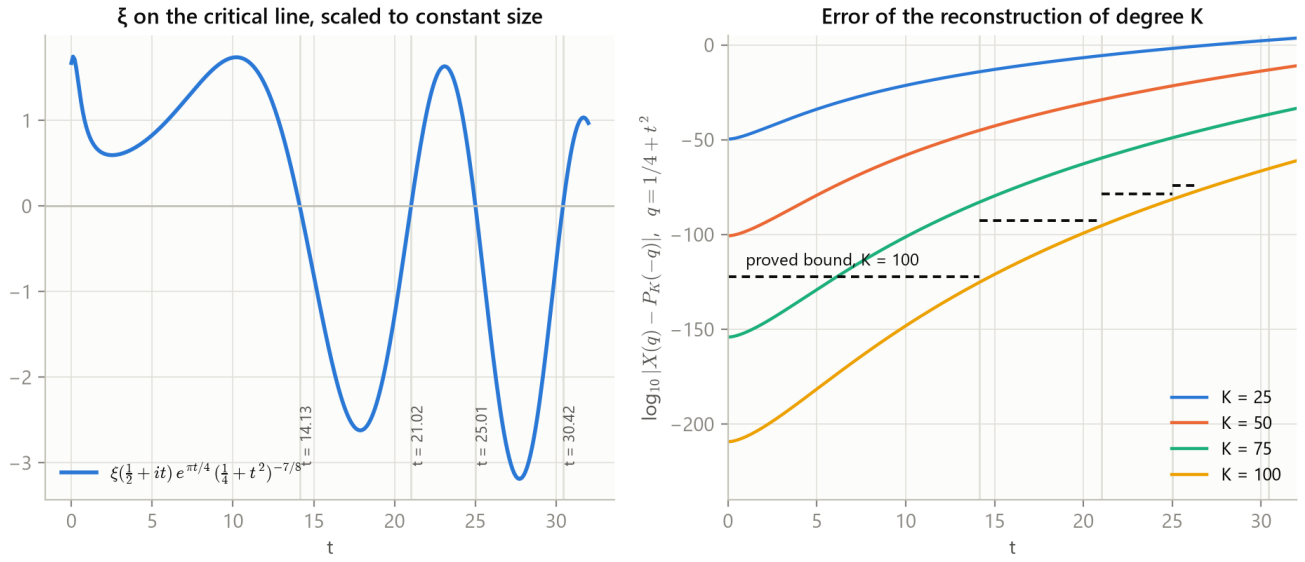

Figure 6: Left: $\xi(\frac{1}{2} + it)$, multiplied by $e^{\pi t/4}(\frac{1}{4} + t^2)^{-7/8}$ to remove the leading Gamma envelope, with its first four zeros. The remaining oscillation is not exactly constant in size. Right: the error $\lvert X(q) - P_K(-q)\rvert$ along the critical line for $K = 25, 50, 75, 100$, computed in 360-digit arithmetic. Dashed steps: the proved bounds for $K = 100$ on the disks of the table.

The exponent $\frac{7}{8}$. On the critical line put $A(t) = q\,\pi^{-1/4}\left|\Gamma(\frac{1}{4} + \frac{it}{2})\right|/2$, so that $\lvert X(q)\rvert = A(t)\,\lvert\zeta(\frac{1}{2} + it)\rvert$ exactly. Stirling's formula [13, §5.11] gives

$$A(t) \sim \left(\frac{\pi}{2}\right)^{1/4} q^{7/8} e^{-\pi t/4}, \qquad t \to +\infty,$$

which is the envelope removed in Figure 6. The polynomial factor $\frac{1}{2}s(s-1)$ supplies the power q^1, and the Gamma factor supplies $q^{-1/8}$.

The same $1-\frac{1}{8}$ is the constant in the smooth count of zeros. Let $\theta(t) = \operatorname{Im}\log\Gamma(\frac{1}{4}+\frac{it}{2}) - \frac{t}{2}\log\pi$, continuous with $\theta(0) = 0$, and let $N_0(t)$ count the zeros with ordinate in $(0, t]$, with multiplicity. Then

$$N_0(t) = 1 + \frac{\theta(t)}{\pi} + S(t), \qquad \frac{\theta(t)}{\pi} = \frac{t}{2\pi}\log\frac{t}{2\pi e} - \frac{1}{8} + O\Big(\frac{1}{t}\Big),$$

where $S(t) = \pi^{-1}\arg\zeta(\frac{1}{2}+it)$ is continued from $\arg\zeta(2) = 0$ along $2 \to 2+it \to \frac{1}{2}+it$. At the ordinate of a zero, N_0 and S take the mean of their one-sided limits [13; 19, §2]. The $+1$ in the count also comes from the polynomial factor: $s(s-1)$ turns through the angle π on the way from $s = 2$ to the critical line. So the smooth constant is $\frac{7}{8}$. The amplitude and the count read the same completion, one by size and one by phase. Neither says anything about where the zeros are.

6.2 From a truncation bound to a certified value

The table bounds the error of the exact interpolating polynomial. A computed evaluation also carries coefficient error and arithmetic error. If $|\hat{\eta}_n - \eta_n| \le \varepsilon_n$, then

$$\big|\widehat{P}_K(-q) - X(q)\big| \le E_{\text{trunc}}(q) + \sum_{n=0}^{K} \varepsilon_n \left|\binom{-q}{n}\right| + E_{\text{arith}}(q).$$

On $|q| \le 201$ the middle term is at most $\sum_{n\le 100}\varepsilon_n\binom{200+n}{n}$. By the hockey-stick identity,

$$\sum_{n=0}^{100}\binom{200+n}{n} = \binom{301}{100} = 6.2270\ldots\times 10^{81}.$$

So coefficient enclosures of width ε contribute at most $\varepsilon\binom{301}{100}$ on that disk.

The plotted values in Figure 6 are high-precision evaluations, not certified values. The coefficients were computed through $n = 128$ at 360 digits. They were compared through $n = 120$ with an independent 420-digit computation, with maximum relative discrepancy about 2.1×10^{-76}. Near a zero, a small absolute error does not give a small relative error.

6.3 A certified polynomial

The coefficient enclosures have been computed for $n \le 100$ [17]. Each node s_j, $1 \le j \le 100$, was bracketed by dyadic rationals from an integer square root. Each sample $F(j) = \xi(s_j)$ was then enclosed in interval arithmetic at 1400 bits [21], with $F(0) = \frac{1}{2}$ supplied exactly.

- **The zeta factor.** It is computed by Euler–Maclaurin summation with $D = 300$ terms and $M = 250$ corrections. The remainder obeys

$$|E_{\text{EM}}| \le \frac{4\,s^{\overline{2M}}}{(2\pi)^{2M}}\cdot\frac{D^{1-s-2M}}{s+2M-1},$$

  because the periodic Bernoulli function satisfies $|\widetilde{B}_{2M}| \le |B_{2M}| < 4\,(2M)!/(2\pi)^{2M}$ [13, §§2.10, 24.9].
- **The Gamma factor.** It is computed by Stirling's series after shifting the argument by 400. For real arguments the remainder is bounded by the first omitted term [13, §5.11].

Each sample interval was then widened by a relative 2^{-1350}. The difference table was propagated in exact rational arithmetic, and each coefficient was given an exact dyadic centre $\hat{\eta}_n$. Every interval is strictly positive, and uniformly in $0 \le n \le 100$

$$|\eta_n - \hat{\eta}_n| < 10^{-376}, \qquad \frac{|\eta_n - \hat{\eta}_n|}{\eta_n} < 10^{-171},$$

even at the smallest coefficient, $\eta_{100} = 1.10279\ldots \times 10^{-205}$. Define the exact rational polynomial

$$\widehat{X}_{100}(q) = \sum_{n=0}^{100} (-1)^n \hat{\eta}_n \frac{q^{\overline{n}}}{n!}.$$

Its error splits into the truncation bound of §6.1, $4.68854\ldots \times 10^{-123}$, and the coefficient term of §6.2, $3.93\ldots \times 10^{-295}$. Their exact rational sum is strictly below the target:

$$\sup_{|q|\le 201} \left|X(q) - \widehat{X}_{100}(q)\right| < 4.689 \times 10^{-123}.$$

An independent verifier written with Python integers and fractions alone checks the following:

- the bracketing of every node;
- the signed propagation $\eta_n = \sum_j (-1)^{n-j}\binom{n}{j} F(j)$ from the exported sample intervals;
- the centres and the whole error budget.

It accepts the certificate and rejects a copy with one coefficient's sign changed. The trusted numerical input is the interval enclosure of exp, log and π at the nodes. The analytic input is §4 and the two remainder bounds.

Three further checks support the enclosures:

- Recomputing every sample with different summation parameters gives intervals that overlap the originals.
- Each pair of intervals contains an independent 460-digit value.
- Euler's values $\xi(2), \ldots, \xi(10)$ of §2.2 lie inside their sample intervals.

An earlier independent enclosure, made with Arb [18] at 1200 bits, reached the same final bound.

The statement concerns the polynomial with the full exact centres. It does not cover shortened decimal coefficients, the plotted values of Figure 6, or a floating-point evaluation of $\widehat{X}_{100}$, which needs its own rounding bound. The earlier 360-digit computation was compared with the centres in two places. Its printed values of $\eta_0, \ldots, \eta_7$ agree to their 26 digits, and its stored logarithms of η_n for $n \le 100$ agree to double precision. It is not used in the certificate.

The certificate, both programs, a parameter cross-check and the reproduction notes form the supplement to this paper.

7. Four averaging rules

Burnol's framework has a stationary case: one normalized form L used at every step [3, Proposition 18]. It produces the unique monic Appell sequence $A_0 = 1$, $A_n' = nA_{n-1}$, $L(A_n) = 0$ for $n \ge 1$, and the finite expansion

$$f(z) = \sum_{j=0}^{K} L\big(f^{(j)}\big)\frac{A_j(z)}{j!} + E_{K+1}(f)(z), \qquad E_{K+1}(f) = I^{K+1}\big(f^{(K+1)}\big),$$

where $I\psi = \Psi - L(\Psi)$ for an antiderivative Ψ of ψ.

- **Polynomials.** The expansion is exact once K reaches the degree.
- **Other functions.** An infinite expansion holds only when the remainder tends to zero, and being entire is not enough. For the uniform form on $[0, 1]$ and $f(z) = e^{2\pi i z}$, every coefficient $L(f^{(j)}) = (2\pi i)^j \int_0^1 e^{2\pi i z}\, dz$ vanishes, yet $f(0) = 1$. Burnol's convergent infinite expansion, his Theorem 4, concerns his particular block-directed sequence of measures.

- **The folded ξ.** Its Newton expansion converges by Theorem A, independently of this.

The form determines the polynomials. Four choices of form show where the simplex basis sits (Figure 7).

form L	moments $L(z^n)$	degree-two member	expansion
point mass δ_0	0^n	$z^2/2$	Taylor
uniform on $[0,1]$	$1/(n+1)$	$(z^2 - z + \frac{1}{6})/2$	Euler–Maclaurin (Bernoulli)
triangle $2(1-z)$ on $[0,1]$	$1/T_{n+1}$	$(z^2 - \frac{2}{3}z + \frac{1}{18})/2$	triangular Bernoulli
splines $\delta_0, M_1, M_2, \ldots$ (non-stationary)	B-spline moments	$T(z) = z(z+1)/2$	Newton / simplex

The triangle. The measure $2(1-z)\,dz$ is the triangle of area one on $[0,1]$, and its moments are the reciprocal triangular numbers:

$$\int_0^1 z^n\, 2(1-z)\, dz = \frac{2}{(n+1)(n+2)} = \frac{1}{T_{n+1}}.$$

Summing the moments means applying the form to the geometric series:

$$\sum_{n\geq 1} \frac{1}{T_n} = \int_0^1 \frac{2(1-z)}{1-z}\, dz = 2.$$

The pole of $1/(1-z)$ at $z = 1$ is exactly cancelled by the vanishing edge of the triangle. That is the whole reason the reciprocal triangular numbers sum to 2. More generally, the simplex measure $k(1-z)^{k-1}dz$ has moments $1/p_k(n+1)$, with p_k the simplex polynomial of §3.1, and the same computation gives $\sum_{n\geq 1} 1/p_k(n) = k/(k-1)$ for $k > 1$.

The stationary Appell family of the triangle has generating function

$$\sum_{n\geq 0} A_n(z)\frac{w^n}{n!} = \frac{w^2 e^{zw}}{2(e^w - 1 - w)}.$$

It obeys Bernoulli's recursion with the counting numbers replaced by triangular numbers:

$$\sum_{k=0}^{n} \binom{n}{k} \frac{A_{n-k}(z)}{T_{k+1}} = z^n.$$

This gives $A_1 = z - \frac{1}{3}$, $A_2 = z^2 - \frac{2}{3}z + \frac{1}{18}$ and $A_n(0) = 1, -\frac{1}{3}, \frac{1}{18}, \frac{1}{90}, -\frac{1}{270}, \ldots$. These are the hypergeometric Bernoulli polynomials of order 2, in the sense of Hassen and Nguyen [4, (1.5)–(1.9), Theorem 2.1]. The family is classical; its place in the simplex ladder is what is read here.

Mean and variance. For any stationary form with mean a and variance v,

$$A_2(z) = (z-a)^2 - v.$$

In Figure 7 each parabola's vertex sits at the form's mean, at depth $-v/2$. For the uniform form $v = \frac{1}{12}$, and for the triangle $v = \frac{1}{18}$.

A nondegenerate positive form has no positive inverse. The inverse of translation averaging has exponential coefficients α_n given by $1/L(e^{zw}) = \sum \alpha_n w^n/n!$. For any probability measure with variance v,

$$\det\begin{pmatrix} \alpha_0 & \alpha_1 \\ \alpha_1 & \alpha_2 \end{pmatrix} = -v.$$

For the triangle the coefficients are $1, -\frac{1}{3}, \frac{1}{18}, \ldots$ and the determinant is $-\frac{1}{18}$. When $v > 0$, as here, the coefficients are not the moments of any positive measure. The condition $v > 0$ is needed: for a point mass δ_a, translation averaging is $f(z) \mapsto f(z+a)$, and its inverse preserves positivity. The inverse of dilation averaging, with reciprocal moments $1, 3, 6, \ldots$, fails in the same way, with determinant -3 [5, Dossier §103.2]. In both cases the positivity of the reference measure does not pass to its inverse. §8 meets the same obstruction in a sharper form.

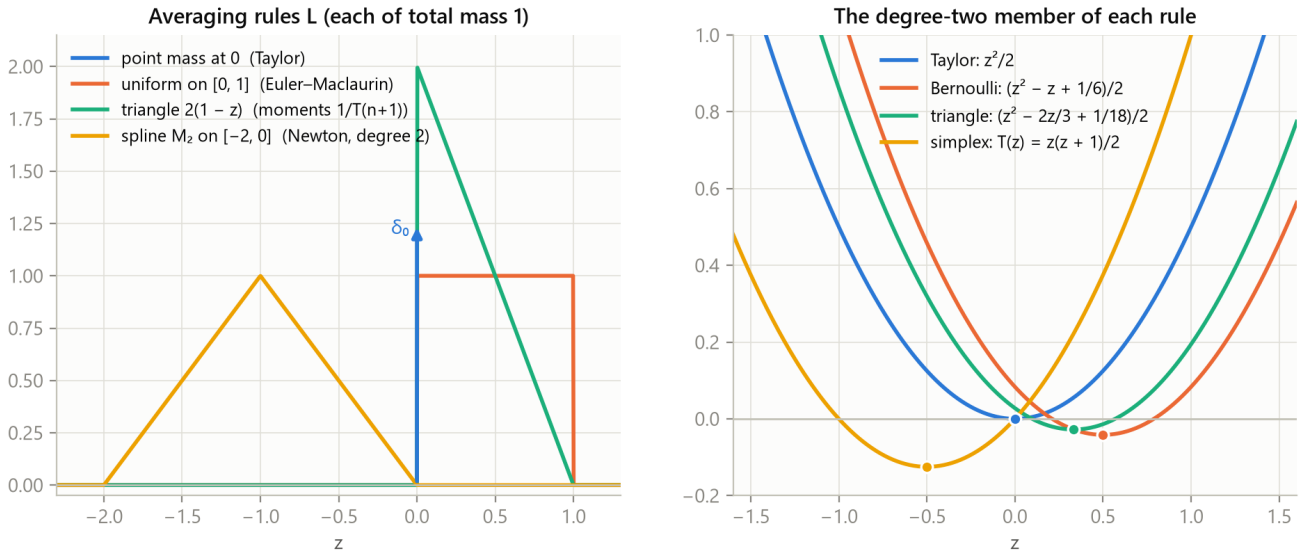

Figure 7: Left: four averaging rules, each of total mass one. Right: the degree-two member that each produces. The stationary rules give $A_2(z)/2! = (z-a)^2/2 - v/2$, with vertex at the mean and depth set by the variance. The simplex rule gives $T(z)$.

The discrete law and its entropy. Halving the reciprocal triangular numbers gives a probability law on the positive integers,

$$\mu_n = \frac{1}{2T_n} = \frac{1}{n(n+1)} = \frac{1}{n} - \frac{1}{n+1},$$

whose total mass telescopes to one. Its entropy in natural units is a sum over the even zeta values:

$$H = -\sum_{n\geq 1} \mu_n \ln \mu_n = -2\sum_{k\geq 1} \zeta'(2k) = \ln 2 + 2\sum_{k\geq 1} \frac{\zeta(2k)-1}{2k-1} = 2.0462774528\ldots,$$

that is 2.9521543 … bits. For the first equality, write $-\mu_n \ln \mu_n = \ln\big(n(n+1)\big)\big(\frac{1}{n} - \frac{1}{n+1}\big)$ and collect the coefficient of each $\ln j$. It is $\frac{1}{j-1} - \frac{1}{j+1} = \frac{2}{j^2-1}$, and expanding $\frac{1}{j^2-1} = \sum_{k\geq 1} j^{-2k}$ gives $\sum_{j\geq 2} \frac{2\ln j}{j^2-1} = -2\sum_k \zeta'(2k)$. For the second, $\sum_k \frac{j^{-2k}}{2k-1} = \frac{1}{j}\operatorname{artanh}\frac{1}{j} = \frac{1}{2j}\ln\frac{j+1}{j-1}$, and summation by parts returns the same series in $\ln j$.

This is the classical entropy of the Lüroth map, whose branches have lengths μ_n [20]. The direct sum converges like $(\ln K)/K$. The zeta form gains about 0.6 digits per term, since $\zeta(2k) - 1 \approx 4^{-k}$ (Figure 8). The law μ_n lives on the integers. It is distinct from the continuous triangle $2(1-z)\,dz$ above, whose moments are the same reciprocals.

The fold carries the two-outcome case. On the real segment $0 \leq s \leq 1$, the coordinate $q = s(1-s)$ is the variance of a coin that shows heads with probability s. The coin's entropy $h(s) = -s\ln s - (1-s)\ln(1-s)$

satisfies

$$h''(s) = -\frac{1}{s(1-s)} = -\frac{1}{q}, \qquad 0 < s < 1.$$

Its maximum, $\ln 2$, sits at the vertex $q = \frac{1}{4}$, where the real branch of the fold meets the critical-line branch.

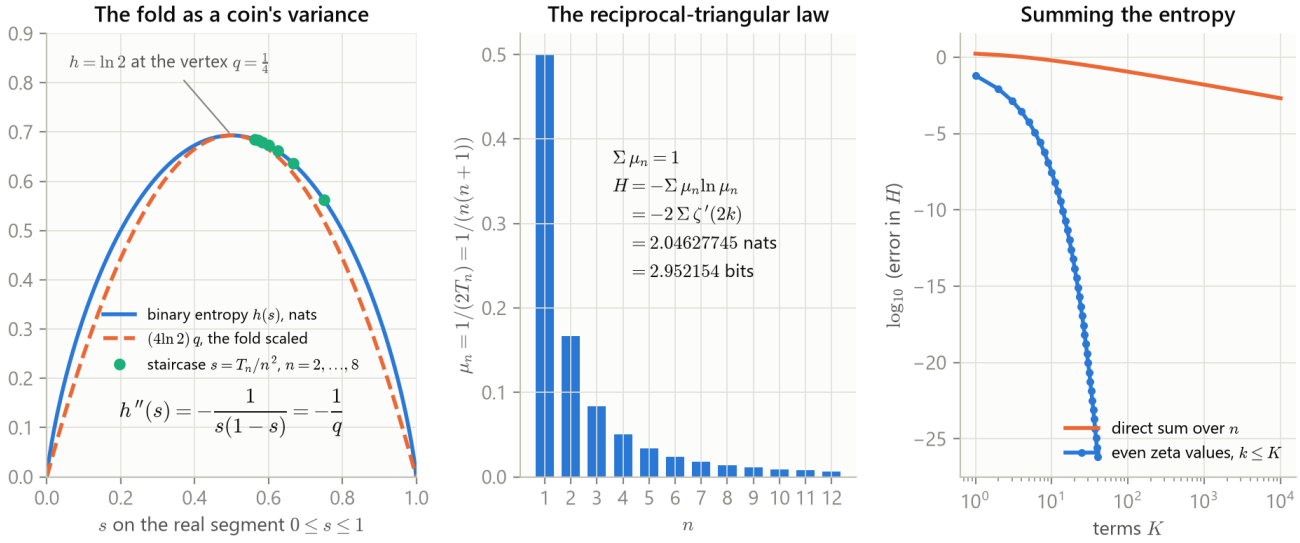

Figure 8: Left: on the real segment the fold $q = s(1-s)$ is a coin's variance. The binary entropy $h(s)$, in nats, meets the scaled fold $(4\ln 2)\,q$ at the vertex $q = \frac{1}{4}$, and $h'' = -1/q$ for $0 < s < 1$. The staircase points $s = T_n/n^2$ of §2.3 are marked. Centre: the reciprocal-triangular law $\mu_n = 1/(2T_n)$ and its entropy. Right: the error in H after K terms, for the direct sum over n and for the sum over the even zeta values.

8. What the expansion does not decide

8.1 Two coefficient systems

The Taylor coefficients in the normalization of [5, Reading Volume (12.9)] are

$$\frac{F(x)}{\xi(1)} = \sum_{k\ge 0} \tau_k x^k, \qquad \xi(1) = \tfrac{1}{2}.$$

They are connected to the Newton coefficients by Stirling numbers:

$$\eta_n = \frac{n!}{2} \sum_{k\ge n} \left\{ {k \atop n} \right\} \tau_k, \qquad \tau_k = 2 \sum_{n\ge k} (-1)^{n-k} \left[{n \atop k} \right] \frac{\eta_n}{n!},$$

where $\left\{ {k \atop n} \right\}$ are the Stirling numbers of the second kind and $\left[{n \atop k} \right]$ those of the first kind, both nonnegative. Both identities converge, and either sequence recovers the other. The forward map preserves positivity; the inverse map has alternating signs.

8.2 The determinant criterion

Under the Riemann hypothesis, every zero of F lies on the negative real axis at $x = -q_\rho \le -\frac{1}{4}$. An entire function of order below one with only negative zeros has Taylor coefficients forming a Pólya frequency sequence. Conversely, such a sequence forces the zeros to be real and negative. Since ξ has no real zeros in $(0, 1)$, this gives:

RH holds if and only if every minor of the Toeplitz matrix $[\tau_{i-j}]_{i,j\geq 0}$ (with $\tau_k = 0$ for $k < 0$) is nonnegative [5, (12.9)], [15].

The word *every* matters. The leading sections $\det[\tau_{i-j}]_{i,j<k}$ are lower triangular with unit diagonal, so they all equal 1 and carry no information. The content lies in the other minors.

Theorem A gives $\eta_n > 0$, and the positive kernel gives $\tau_k > 0$; neither reaches the minors. Small examples show that no generic shortcut works:

- **Positive Newton data, complex zeros.** $F(x) = 1 + 2x + 2x^2$ has Newton coefficients $(1, 4, 4)$, a Pólya frequency sequence with generating polynomial $(1 + 2w)^2$. Yet F has nonreal zeros (discriminant -4).
- **Negative zeros, complex truncation.** $F(x) = (1 + x)^3$ has only negative zeros, but its degree-two Newton interpolant is $1 + x + 6x^2$, with discriminant -23.
- **All signs right, one minor wrong.** $X(q) = 2 + \cos\sqrt{q}$ has positive Taylor coefficients $3, \frac{1}{2}, \frac{1}{24}, \frac{1}{720}, \ldots$ for $F(x) = 2 + \cosh\sqrt{x}$, and so, by §3.2, every forward difference is positive. Yet it has nonreal zeros. Rows 1–4 and columns 0–3 of its Toeplitz matrix give

$$\det\begin{pmatrix} \frac{1}{2} & 3 & 0 & 0 \\ \frac{1}{24} & \frac{1}{2} & 3 & 0 \\ \frac{1}{720} & \frac{1}{24} & \frac{1}{2} & 3 \\ \frac{1}{40320} & \frac{1}{720} & \frac{1}{24} & \frac{1}{2} \end{pmatrix} = -\frac{17}{4480}.$$

- **Symmetry and positivity are not enough.** For $a > 0$, multiply $\xi(s)$ by $H_a(s)/H_a(1)$, where $H_a(s) = \cosh(a/4) + \cosh\big(a(s - \frac{1}{2})\big)$. This keeps the reflection, conjugation symmetry, normalization and a positive transform kernel. But it adds zeros on the lines $\mathrm{Re}\, s = \frac{1}{4}$ and $\frac{3}{4}$, at heights $(2j + 1)\pi/a$.

These structural properties alone do not force the minors. The arithmetic source of ξ, the Gamma–prime structure of the explicit formula, is the additional structure this program targets [5].

8.3 The same basis in other hands

The rising-simplex basis has carried ζ before. Maślanka's representation [6] reads

$$(s-1)\zeta(s) = \sum_{k\geq 0} A_k\, p_k\big(1 - \tfrac{s}{2}\big), \qquad A_k = \sum_{j=0}^{k} (-1)^j \binom{k}{j} (2j+1)\,\zeta(2j+2).$$

Its coefficients are Newton differences of the even zeta values. Báez-Duarte proved that it converges for all s [7]. For $1/\zeta$, the analogous coefficients $C_k = \sum_j (-1)^j \binom{k}{j}/\zeta(2j+2)$ give Báez-Duarte's criterion: RH holds if and only if $C_k \ll k^{-3/4+\varepsilon}$ for every $\varepsilon > 0$ [8]. The asymptotics of such differences are treated by Flajolet and Vepstas [9].

These results and the present one share a basis but differ in variable and function. Maślanka's series uses the variable $1 - s/2$ and samples at the even integers. The present series uses the fold $q = s(1 - s)$, the completed function and every integer node j.

Maślanka's reconstruction of ζ is unconditional. RH enters elsewhere in each setting:

- Báez-Duarte's reciprocal-zeta criterion places it in a quantitative decay condition on the C_k.
- The present ordinary-coefficient formulation places it in the full family of Toeplitz minors.

In neither does it lie in the signs of the coefficients.

8.4 A boundary in the literature

A printed condition for ordinary Newton representations, order one and type below π [10, Corollary 2.1], is not sufficient as stated. For $f(z) = 2^z$, which has type $\ln 2 < \pi$, every forward difference at 0 equals 1, and the Newton terms at $z = -1$ are $(-1)^n$, which do not tend to zero. The series $\sum \binom{z}{n}$ converges only for $\operatorname{Re} z > -1$. Theorem A does not rely on that condition: it uses its own contour remainder and the order-$\frac{1}{2}$ growth of F.

9. Around the fold

9.1 Burnol's other theorem: digit sums with modes 91, 991, 9991

Burnol's paper [3], which supplies the averaging framework of §§3 and 7, is about something else: harmonic sums over integers with a prescribed number of occurrences of a digit block. Kempner (1914) showed that $\sum 1/k$ over integers k with no digit 9 converges. Irwin (1916) treated exactly n nines. Let H_n be the sum of $1/k$ over integers whose decimal form has exactly n nines. Computing these sums to 40 digits gives:

- $H_0 = 22.92067661926415034816\ldots$, Kempner's sum, as computed by Baillie [11];
- $H_1 = 23.04428708074784831968\ldots$;
- $H_n \to 10 \ln 10 = 23.0258509\ldots$ as n grows (Farhi [12]).

The gaps fall by $1/91$**.** Burnol proves this structure [3, Theorems 1–2]. For every $n \geq 1$,

$$H_n = 10 \ln 10 + \sum_{j \geq 2} \frac{\alpha_j}{(10^j - 9)^n},$$

absolutely convergent; in base g the moduli $10^j - 9$ become $g^j - g + 1$. The case $n = 0$ needs a separate expansion.

The moduli have a short source. If W counts the digits read through the next 9, then $\Pr(W = k) = 9^{k-1}10^{-k}$ and

$$\mathbb{E}\, 10^{-(j-1)W} = \frac{1}{10^j - 9}$$

[3, (19)]. The first amplitudes $\alpha_2, \alpha_3, \alpha_4$ are positive; they can be computed exactly from Burnol's moment recurrences. So, with $D_n = H_n - 10 \ln 10$, $D'_n = D_n - 91 D_{n+1}$ and $D''_n = D'_n - 991 D'_{n+1}$,

$$\frac{D_n}{D_{n+1}} \to 91, \qquad \frac{D'_n}{D'_{n+1}} \to 991, \qquad \frac{D''_n}{D''_{n+1}} \to 9991,$$

in agreement with the computed sums.

The eigenvectors in Burnol's analysis are the Lebesgue measure and derivatives of singular measures. The dual objects are eigenpolynomials, and the resulting modal expansion is the block-directed Euler–Maclaurin formula of his Part 3, the family to which §7 belongs.

Why $10 \ln 10$**.** Let $Y_n(z)$ be the decimal prefix of $z \in [0, 1)$ before its $(n+1)$-st digit 9. For $n \geq 1$ Burnol's integral representation [3, (14)] reads

$$H_n = 10 \int_{1/10}^{1} \frac{dz}{Y_n(z)}.$$

Here $Y_n(z) \geq \frac{1}{10}$ and $Y_n(z) \uparrow z$ for almost every z, so by dominated convergence $H_n \to 10 \int_{1/10}^{1} dz/z = 10 \ln 10$. In words, the factor 10 is the waiting time for a 9, and $\ln 10$ is one decade of harmonic weight.

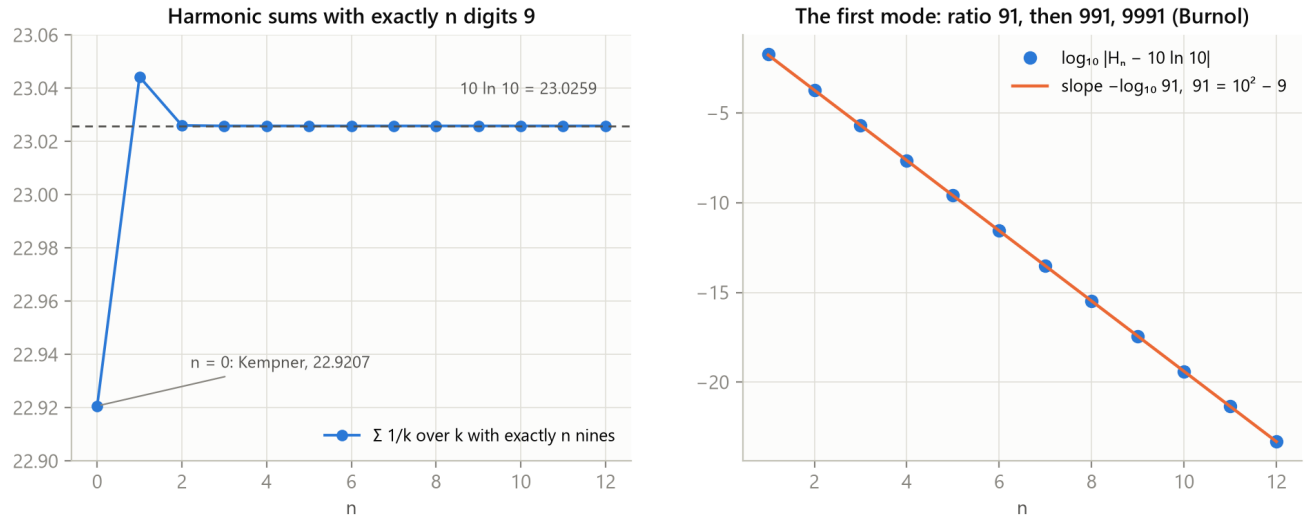

Figure 9: Left: harmonic sums over integers with exactly n nines, from Kempner's $n = 0$ to the limit $10 \ln 10$. Right: $\log_{10} |H_n - 10 \ln 10|$ falls with slope $-\log_{10} 91$, the first of Burnol's modes $1/(10^j - 9)$.

9.2 The even nodes and the zeta ladder

The even-integer nodes of §2.2 carry the Bernoulli ladder $\zeta(2k) = |B_{2k}|(2\pi)^{2k}/(2(2k)!)$. Neighbouring rungs divide to

$$\frac{\zeta(2k+2)}{\zeta(2k)} = \frac{(2\pi)^2}{(2k+1)(2k+2)} \left| \frac{B_{2k+2}}{B_{2k}} \right|.$$

One rung has a decimal face. At $k = 4$, $|B_{10}/B_8| = (5/66)/(1/30) = 25/11$, so before any cancellation

$$\frac{\zeta(10)}{\zeta(8)} = \frac{(2 \cdot 5 \cdot \pi)^2}{9 \cdot 10 \cdot 11} = \frac{(10\pi)^2}{990} = \frac{10}{99}\pi^2.$$

Each factor has a source:

- the 2 is the 2π of Euler's formula;
- $25 = 5 \cdot 5$, where one 5 is the numerator of $B_{10} = 5/66$ and the other is the prime 5 in the denominator 30 of B_8, by the von Staudt–Clausen rule ($5 - 1$ divides 8);
- $9 \cdot 10 = 10!/8!$ comes from the factorials;
- 11 is the prime in the denominator 66 of B_{10} ($11 - 1$ divides 10), while the $2 \cdot 3$ shared by 30 and 66 cancels.

So $100/990$ is the ratio as Euler's formula delivers it, and $10/99$ is what remains after the factorial's 10 cancels against $2 \cdot 5$. That cancellation belongs to this rung: the neighbouring ratios are $\pi^2/10$ and $691\pi^2/6825$. That $990 = 9 \cdot 10 \cdot 11$ is also the triangular number T_{44} is a coincidence of a rarer kind. Among the products $n(n+1)(n+2)$ with $n < 2 \cdot 10^6$, only six are triangular: 6, 120, 210, 990, 185136 and 258474216. At this rung the ladder's own numbers are base ten's $10^3 - 10$. In particular

$$\frac{\pi^{10}}{990} = \frac{189}{2}\zeta(10) = 94.5 + 94.5\left(2^{-10} + 3^{-10} + \cdots\right),$$

so the excess over 94.5 is exactly the scaled zeta tail, about 0.0939873. The scale is not unique: the primitive pair is $\pi^{10}/99 = 945\,\zeta(10)$ and $\pi^8/10 = 945\,\zeta(8)$.

A neighbouring observation is numerical. The fraction $92711567/990 = 93648 + 47/990 = 93648.0\overline{47}$ lies within 1.34×10^{-6} of π^{10}. It is the best approximation to π^{10}, in absolute error, among all denominators up to 990: an intermediate fraction of its continued fraction $[93648; 21, 15, 1, 4, 2, \ldots]$, with 337 the runner-up.

How unusual is this? Take a uniform model for the fractional part, and fix in advance the denominator $d = 990$ and the absolute tolerance $\varepsilon = \pi^{10} - 92711567/990$. The chance of lying within ε of some k/d is then $2d\varepsilon \approx 1/380$. Now search all denominators $d \leq 1000$ at the same tolerance. The chance becomes about 0.687: the measure of the union of the ε-intervals around all fractions with denominator at most 1000, overlaps counted once. In that search a fraction this close is more likely than not. This is a model for one declared finite search, not a distribution established for π. Fixing the product $d\varepsilon$ instead would define a different search. The identity with the scaled zeta tail rewrites the same fractional part and does not explain why it is small. Nothing yet explains why $990\pi^{10}$ lands so near an integer, and none of this is used elsewhere in the paper.

10. Status of the results

statement	status	where
$\eta_n > 0$ for every n; global absolute convergence	proved	§4
contour remainder (4.1) and rational bound (4.2)	proved	§4
the five disk bounds for $K = 100$ (exact interpolant)	proved by exact rational comparison	§6.1
enclosures of $\eta_0, \ldots, \eta_{100}$; $\sup_{\lvert q\rvert \leq 201} \lvert X - \widehat{X}_{100}\rvert < 4.689 \times 10^{-123}$	certified (interval sample enclosures, exact rational verifier)	§6.3
the fold as $q = (1 - J^2)/4$ with $J^2 = 8T(s-1) + 1$; staircase points $q = \frac{1}{4} - 1/(4n^2)$	exact	§2.3
M_n as the shadow of a uniform n-simplex	proved (classical)	§3.2
$n\eta_n^{1/n}/(\ln n)^2 \to e/16$ for unit step; $\lambda e/16$ for each fixed step $\lambda > 0$	proved	§5.2
corrections $-2n\ell_2/\ell_1$ and $2(\ln\frac{2}{\pi} - 1)n/\ell_1$	proved, two-sided	§5.3
$G_n \to 0$, $G_n^{1/n} \to 1$	proved	§5.4
$q^{7/8}$ in the Gamma envelope; smooth constant $\frac{7}{8}$ in $N_0(t)$	classical (Stirling; standard counting identity)	§6.1
coefficients $\eta_0, \ldots, \eta_{128}$; sampled errors in Figure 6	computed through $n = 128$ at 360 digits; compared through $n = 120$ at 420 digits (about 2.1×10^{-76}); the plotted values are not certified	§§5–6
stationary averaging expansions	finite, with remainder; infinite only when the remainder vanishes	§7
simplex basis as Burnol's non-stationary scheme with spline forms	proved (classical ingredients)	§3

statement	status	where
triangular Bernoulli family; $\sum 1/T_n = 2$ from the triangle form	proved; family as in Hassen–Nguyen	§7
inverse-averaging determinants $-v$ (for $v > 0$) and -3	proved	§7
entropy of $\mu_n = 1/(2T_n)$ as sums over $\zeta'(2k)$ and $\zeta(2k)$; $H = 2.04627745\ldots$ nats	proved; classical (Lüroth map)	§7
$h''(s) = -1/q$ for the binary entropy, $0 < s < 1$	exact	§7
$e_k(-\frac{1}{2}) = 1, -\frac{1}{8}, \frac{1}{128}, \ldots$ as the expansion coefficients of $y^{-1/2}\Gamma(1/y + \frac{1}{2})/\Gamma(1/y + 1)$, $y \to 0^+$	proved (classical ingredients)	§2.3
RH $\Leftrightarrow$ all Toeplitz minors of (τ_k) nonnegative	classical equivalence	§8.2
those minors	**open**	§8.2
digit-sum modes $1/(10^j - 9)$ for $n \geq 1$	theorem of Burnol; our values computed to 40 digits	§9.1
$990\pi^{10}$ near an integer	observation; about 0.687 in the declared search $d \leq 1000$; no explanation	§9.2

Acknowledgments and methods

The arguments were developed and cross-examined with several AI systems acting as independent reviewers: ChatGPT (Astra Pro), OpenAI Codex agents, Anthropic's Claude and Google's Gemini. Each proof was read by a second reviewer before it was accepted here. The computations behind the paper:

- **Coefficient tables.** Computed twice, independently, at 360 and 420 digits.
- **Rational bounds.** Checked in exact integer arithmetic.
- **The certificate of §6.3.** Produced with mpmath 1.3.0 interval arithmetic at 1400 bits, and checked by a separate standard-library verifier, including on a deliberately corrupted copy. An earlier enclosure with python-flint 0.9.0 (FLINT 3.6.0) at 1200 bits reached the same bound.
- **Figures.** Drawn from the 360-digit computation.

Every number in this paper was rechecked against those computations, and the claims of §§2, 6.1, 7, 8 and 9 against a separate set of exact checks. Responsibility for the mathematics and its presentation is the author's.

References

1. D. Romik, *Orthogonal polynomial expansions for the Riemann xi function in the Hermite, Meixner–Pollaczek, and continuous Hahn bases*, equations (1.8), (1.11). https://www.math.ucdavis.edu/~romik/data/uploads/papers/riemannxi-final.pdf
2. C. O'Sullivan, *Zeros of Jensen polynomials and asymptotics for the Riemann xi function*, (7.1). https://fsw01.bcc.cuny.edu/cormac.osullivan/Research/xi-revised.pdf
3. J.-F. Burnol, *Block-count constrained harmonic sums: spectral expansion and block-directed Euler–Maclaurin*, arXiv:2609.17045 (2026). Theorems 1–2; Propositions 18, 20, 21; Theorem 4.

4. A. Hassen and H. D. Nguyen, *Hypergeometric Bernoulli polynomials and Appell sequences*, Int. J. Number Theory 4 (2008), 767–774.
5. J. Huckstead, *Triangular n Postmaster: From the Discrete Primitive to the Completed Source Frontier*, Volume I (2026): Reading Volume (12.9); Technical Dossier §103.2.
6. K. Maślanka, *A hypergeometric-like representation of the zeta-function of Riemann*, arXiv:math-ph/0105007.
7. L. Báez-Duarte, *On Maślanka's representation for the Riemann zeta-function*, arXiv:math/0307214 (2003).
8. L. Báez-Duarte, *A sequential Riesz-like criterion for the Riemann hypothesis*, Int. J. Math. Math. Sci. 2005:21, 3527–3537.
9. P. Flajolet and L. Vepstas, *On differences of zeta values*, J. Comput. Appl. Math. (2008); arXiv:math/0611332.
10. K. Ishizaki and Z.-T. Wen, *Binomial series and complex difference equations*, arXiv:1908.11580v2 (2020), §2.6, Corollary 2.1.
11. R. Baillie, *Sums of reciprocals of integers missing a given digit*, Amer. Math. Monthly 86 (1979), 372–374; T. Schmelzer and R. Baillie, *Summing a curious, slowly convergent series*, Amer. Math. Monthly 115 (2008), 525–540.
12. A. J. Kempner, *A curious convergent series*, Amer. Math. Monthly 21 (1914), 48–50; F. Irwin, *A curious convergent series*, Amer. Math. Monthly 23 (1916), 149–152; B. Farhi, *A curious result related to Kempner's series*, Amer. Math. Monthly 115 (2008), 933–938.
13. NIST Digital Library of Mathematical Functions: §2.10 (Euler–Maclaurin), §5.11 (Gamma asymptotics), §24.9 (Bernoulli inequalities) and §25.4 (the completed zeta function). https://dlmf.nist.gov
14. J. Huckstead, *Project 51: Reading the Record Across Rules* (2026); *Cayley–Casimir Bridge to Exact Semidiscrete Flux Scattering* (2026). Companion papers on recovering a function from a specified reading.
15. M. Aissen, I. J. Schoenberg and A. M. Whitney, *On the generating functions of totally positive sequences I*, J. Analyse Math. 2 (1952), 93–103; A. Edrei, *On the generating functions of totally positive sequences II*, J. Analyse Math. 2 (1952), 104–109.
16. H. B. Curry and I. J. Schoenberg, *On Pólya frequency functions IV: the fundamental spline functions and their limits*, J. Analyse Math. 17 (1966), 71–107.
17. *Supplement to this paper*: the coefficient certificate (`certificate.json`), its producer (`build_certificate.py`), the independent verifier (`verify_certificate.py`), a parameter cross-check (`crosscheck_parameters.py`) and reproduction notes (`REPRODUCE.md`).
18. F. Johansson, *Arb: efficient arbitrary-precision midpoint-radius interval arithmetic*, IEEE Trans. Comput. 66 (2017), 1281–1292; python-flint documentation, https://python-flint.readthedocs.io.
19. R. P. Brent, D. J. Platt and T. S. Trudgian, *Accurate estimation of sums over zeros of the Riemann zeta-function*, Math. Comp. 90 (2021), 2923–2935, §2. doi:10.1090/mcom/3652
20. W. Bosma, K. Dajani and C. Kraaikamp, *Entropy quotients and correct digits in number-theoretic expansions*, in *Dynamics & Stochastics*, IMS Lecture Notes–Monograph Series 48 (2006), 176–188, Example 2.3(iii). doi:10.1214/074921706000000202
21. F. Johansson and others, *mpmath: a Python library for arbitrary-precision floating-point arithmetic*, version 1.3.0 (2023), interval arithmetic in `mpmath.iv`. https://mpmath.org